Catal Lett (2011) 141:391–399
DOI 10.1007/s10562-010-0511-0

Selective Production of 2-Phenylhexane from Benzene and *n*-Hexane Over Pt- and Ga-Modified Zeolites

Nadiya Danilina · Elisabeth L. Payrer · Ekaterina Troussard · Jeroen A. van Bokhoven

Received: 25 May 2010 / Accepted: 22 November 2010 / Published online: 14 December 2010

Abstract Alkylation of benzene with *n*-hexane was performed over H-ZSM-5 and monometallic Ga- and Pt- and bimetallic Ga- and Pt-modified ZSM-5. The influence of the particle size and the method of incorporation of Ga (during hydrothermal synthesis, by solid-state ion exchange, or by liquid-state ion exchange) was determined. The presence of Pt and well-dispersed extraframework Ga in H-ZSM-5 increased the selectivity in alkylation and suppressed cracking reactions. Well-dispersed Pt particles led to better catalytic performance. The method of Ga incorporation played an important role in obtaining higher selectivity to alkylation products and in the suppression of side reactions. Up to 93% selectivity in alkylation (of which >95% was to 2-phenylhexane) was reached over 2 wt% Pt/H-Ga^{f}ZSM5, in which Ga occupied framework positions. We propose that the close proximity of very small Pt nanoparticles and Ga–(OH)–Si acid sites results in the optimal bifunctional catalyst for selective production of 2-phenylhexane from benzene and *n*-hexane. During the reaction, the catalyst deactivated, most probably due to the sintering of the Pt particles.

Keywords Alkylation · Zeolite · ZSM-5 · Ga · Pt · Particle size

1 Introduction

High selectivity to linear phenylalkanes is a very important issue in the production of linear phenylalkanesulfonates (alkylbenzenesulfonates) [1, 2]. Phenylalkanesulfonates are surfactants and are the main ingredient of many synthetic detergents [2]. Linear phenylalkanes are still the most cost-effective detergent intermediates. Phenylalkanesulfonates obtained from 2-phenylalkanes have the highest degree of biodegradability (>90%) among phenylalkanes [2]. Therefore, efficient and selective synthesis of 2-phenylalkanes is required to produce biodegradable and environmentally friendly surfactants. About 80% of linear phenylalkanes manufactured worldwide are produced by UOP technology and the Pacol process [3] to give alkylation of benzene with dehydrogenated *n*-C_{10}–C_{13} alkanes in the presence of hydrofluoric acid. Solid acid catalysts, such as zeolites, supported aluminum chloride, clays, and various metal oxides, are emerging and will, with time, replace the corrosive and toxic hydrofluoric acid process. To date, however, only the Detal process [1], which uses a heterogeneous catalyst, fluorided silica–alumina [4], has been commercialized. The selectivity to 2-phenylalkane in the Pacol process is about 15–18% at a conversion of almost 100%; in the Detal process, it surpasses 25% at almost full conversion [1]. It is certainly possible to improve the selectivity to the desirable 2-phenylalkane.

In general, aromatics are alkylated with olefins to obtain phenylalkanes. However, replacing olefins with alkanes decreases the cost of the feed and may enhance catalytic stability. Because it is much more difficult to activate

Electronic supplementary material The online version of this article (doi:10.1007/s10562-010-0511-0) contains supplementary material, which is available to authorized users.

N. Danilina · E. L. Payrer · E. Troussard · J. A. van Bokhoven (✉)
Institute for Chemical and Bioengineering, ETH Zurich, Wolfgang-Pauli-Str. 10, 8093 Zurich, Switzerland
e-mail: j.a.vanbokhoven@chem.ethz.ch

E. Troussard · J. A. van Bokhoven
Laboratory for Energy and Environment, Paul Scherrer Institute, WLGA/135, 5232 Villigen, Switzerland

alkanes than olefins, super acids [5] or bifunctional catalysts [8, 11, 12] are required. Although very high conversion and selectivity were reached with superacids, such processes have many environmental drawbacks. Solid acids, such as zeolites [6–17], often modified with Pd, Pt, or Ga [2, 3, 12], do not have these drawbacks. However, they have low activity and selectivity towards alkylaromatic products at moderate reaction temperature (vide infra). Ethane [7, 12, 14–16, 18, 19] and propane [7–11, 13] have been used to date to alkylate aromatics over zeolite-based catalysts. A selectivity of 80% to ethylbenzene was obtained over Pt/H-ZSM-5 by alkylation of benzene with ethane at a conversion of about 2% in ethane [16]. Alkylation with propane over Pt/H-ZSM-5 resulted in up to 60% selectivity to cumene and *n*-propylbenzene at about 7% propane conversion [8]. At higher conversion, the selectivity decreased significantly. Over H-ZSM-5 impregnated with Ga, about 10% selectivity to cumene and *n*-propylbenzene were attained at a conversion of 2% [11]. Both activity and selectivity to alkylated products increased over bimetallic Pt- and Ga-modified ZSM-5, Pt/H-GaZSM-5, with Ga in the framework positions [10]. Ga ions and Pt particles promote dehydrogenation, and Pt suppresses the formation of coke [7, 11].

Our study demonstrates that almost 90% selectivity to 2-phenylhexane can be achieved in the direct aromatic alkylation with *n*-hexane at reasonable conversion ($\sim$20%) by optimizing reaction conditions and modifying zeolites with Ga and/or Pt. We show that the zeolite structure, the metal and its particle size, and the way in which the metal is incorporated all have a strong effect on the activity and, in particular, on the selectivity to alkylaromatics.

2 Experimental

2.1 Catalysts

Zeolite H-ZSM5 (Si/Al = 25) was obtained from Zeochem (PZ-2/50 H), Switzerland. H-Ga^{f}ZSM5, the protonic form of Ga^{f}ZSM-5 (Ga in the framework, Al-free), was kindly provided by Jeff Miller (Amoco Research Centre, USA). H-ZSM5 was modified with Pt and Ga by wet impregnation or by ion exchange. For the solid-state ion exchange of Ga into H-ZSM5, Ga_2O_3 (ABCR, 99.99%) and the zeolite were mixed (1:1), suspended in *n*-hexane, and heated to 450 °C in a flow of nitrogen (15 mL/min). The sample was referred to as Ga^{s}/H-ZSM5. For the liquid-state ion exchange, 1 g of H-ZSM5 was dispersed in 10 mL 0.15 M aqu. $Ga(NO_3)_3$ (Acros Organics, 99.9998%). After stirring for 15 min, the catalyst was filtered, washed with 1 L deionized water, and dried at 125 °C for 5 h with 1 °C/min, then at 225 °C for 3 h with 1 °C/min, and subsequently, calcined at 300 °C for 8 h with 0.2 °C/min in the air flow (30 mL/min). Ga^{i}/H-ZSM5 was obtained. All Ga-containing samples were reduced at 400 °C with 0.5 °C/min for 1 h in pure hydrogen before they were used as a catalyst or a support. To load with Pt, 2 g of the zeolite (H-ZSM5, H-Ga^{f}ZSM5, Ga^{s}/H-ZSM5, or Ga^{i}/H-ZSM5) were suspended in 16 mL deionized water and 0.4 mL NH_4OH; 0.08 g $[Pt(NH_3)_4](NO)_2$ (Aldrich, 99.995%) were dissolved in 4 mL water and 0.16 mL NH_4OH. The mixtures were stirred for 15 min, after which the Pt-precursor mixture was stirred into the zeolite suspension. After stirring for another 15 min, the catalysts were filtered, washed with 1 L deionized water, and dried at 125 °C for 5 h with 1 °C/min, and then at 225 °C for 3 h with 1 °C/min. The catalysts were then calcined at 300 °C for 8 h with 0.2 °C/min in a flow of air (30 mL/min). Pt/H-ZSM5, Pt/H-Ga^{f}ZSM5, PtGa^{s}/H-ZSM5, and PtGa^{i}/H-ZSM5 were obtained. All the Pt-containing samples were reduced in pure hydrogen (20 mL/min) at 250 °C for 2 h with 1 °C/min. To obtain larger Pt particles on H-Ga^{f}ZSM5, the heating rate was increased to 5 °C/min. The resulting sample is referred to as Pt$_b$/H-Ga^{f}ZSM5.

2.2 Catalyst Characterization

X-ray powder diffraction (XRD) was conducted on a STOE STADI-P2 diffractometer in transmission mode with a flat sample holder and Ge-monochromated Cu Kα_1 radiation. The instrument was equipped with a position-sensitive detector with a resolution of about 0.01° in 2θ.

Nitrogen sorption measurements were performed at the temperature of liquid nitrogen on a Tristar 3000 apparatus of Micromeritics. Before the measurements, the samples were degassed at 10 mPa and 250 °C for at least 2 h. The surface area was determined by the BET method and the specific pore volume by the t-plot method.

Atomic absorption spectroscopy (AAS) was performed on a Varian SpectrAA 220 FS spectrometer to determine elemental constitution. The samples were dissolved in an HF/HNO_3/water matrix overnight. Quantification of aluminum was done by the standard addition method. For other elements, individual calibration curves were measured and used for quantification.

Transmission electron micrographs (TEM) were obtained on a Philips CM30 microscope with a point resolution of 0.2 nm at 300 kV. Scanning transmission electron microscopy (STEM) was performed with a Tecnai F30 microscope operating with a field-emission cathode at 300 kV. STEM images, obtained with a high-angle annular dark-field (HAADF) detector, revealed the metal clusters with a bright contrast (Z contrast). To prepare samples for TEM and STEM, they were ground, dispersed in ethanol, and deposited onto a holey carbon film supported on a copper grid.

^{71}Ga MAS NMR experiments were carried out on a Bruker Avance 700 NMR spectrometer with a 2.5 mm double-resonance probe-head. The resonance frequency for ^{71}Ga was 91.5 MHz, and the pulse length was 6 µs. All spectra were obtained at a spinning speed of 15 kHz and had a recycle delay of 1 s. The ^{71}Ga chemical shifts were referenced to 1 M $Ga(NO_3)_2{\cdot}8H_2O$.

The Fourier-transform infrared spectra (FTIR) were recorded on a Biorad Excalibur FTS 3000 IR spectrometer in transmission mode. The spectrometer was equipped with a MCT detector. The spectra were measured at a resolution of 4 cm^{-1} in the range of 1000–3500 cm^{-1}. The sample was pressed into a self-supporting pellet, which was then activated at 500 °C for 1 h in vacuum. The absorption was normalized by the intensity of the structural zeolite band at 1880 cm^{-1}.

2.3 Catalytic Tests

Reactions were performed in PEEK-lined 25-mL Berghof autoclaves BR-25. About 60 mg of the catalyst were transferred to the reactor and covered with benzene (Sigma-Aldrich, puriss.), which was dried over a molecular sieve (ZEOCHEM® Purmol from Uetikon Chemie AG). The alkylation of benzene with *n*-hexane (Acros Organics, 97%, extra dry over molecular sieve) was carried out in a batch reactor between 150 and 220 °C at autogenous or N_2 pressure between 1 and 30 bar and a benzene-to-*n*-hexane (B/H) ratio between 0.5 and 10. The reaction conditions were optimized over H-ZSM5. The best compromise between the conversion of *n*-hexane and selectivity in alkylation was found under the following conditions: 205 °C, autogenous pressure, and a B/H ratio of one. The mixture was stirred at 1250 rpm throughout the run, which was determined to be sufficiently fast. To compare the selectivities over different catalysts at similar conversion, the reaction time was varied between 16 and 27 h. For the time-resolved study, independent reactions were stopped after 15 min, 0.5, 1, 1.5, 2.5, 3.5, 16, 20, and 24 h. The liquid products were analyzed in a GC-MS setup equipped with an HP-5MS column (Agilent Technologies). The amount of the gas and solid products was calculated from the molar carbon balance. The presented catalytic results are mean values of up to three independent experiments. The relative standard deviation was about 7%. The stability of Pt/H-Ga^{f}ZSM5 was evaluated by performing alkylation over the recycled catalyst. The spent catalyst was regenerated by calcination in air followed by reduction in a hydrogen flow according to the procedure applied for the activation of the fresh catalyst. The sample was referred to as Pt/H-Ga^{f}ZSM5r.

3 Results

3.1 Characterization

Ga was introduced into extraframework positions by liquid-state ion exchange (Ga^i/H-ZSM5) or by solid-state ion exchange (Ga^s/H-ZSM5) and into framework positions during hydrothermal synthesis (H-Ga^{f}ZSM5). The samples were modified with Pt nanoparticles. All the samples were of the MFI framework type and did not lose crystallinity upon ion exchange (Figure S1, supporting information). For Ga^s/H-ZSM5 and PtGa^s/H-ZSM5, reflections at around 32, 35, and 65 2θ ° appeared, which are attributed to Ga_2O_3.

Table 1 lists the characteristics of all the zeolite samples. There was 0.3–9.6 wt% Ga in the Ga-containing samples. The lowest amount of Ga was introduced by

Table 1 Characteristics of the zeolite samples

Entry	Catalyst	Ga (wt%)	Pt (wt%)	Metal particle size (nm)	S_{BET} (m^2/g)	S_{ext} (m^2/g)	V_{micr} (cm^3/g)
1	H-ZSM5	–	–	–	400	125	0.12
2	Pt/H-ZSM5	–	2.3	1.6 (Pt)	370	60	0.13
3	Ga^i/H-ZSM5	0.3	–	3.8 (Ga)	350	120	0.10
4	Ga^s/H-ZSM5	9.6	–	–	300	100	0.09
5	H-Ga^{f}ZSM5	2.1	–	–	395	155	0.10
6	PtGa^i/H-ZSM5	0.3	2.3	1.0 (Pt)	355	115	0.10
7	PtGa^s/H-ZSM5	9.6	2.6	1.0 (Pt)	310	100	0.09
8	Pt/H-Ga^{f}ZSM5	2.1	1.8	0.7 (Pt)	360	90	0.11
9	Pt$_b$/H-Ga^{f}ZSM5	2.1	2.0	8.7 (Pt)	350	95	0.10
10	Pt/H-Ga^{f}ZSM5r	2.1	1.9	1.0[a]; 28[b] (Pt)	345	95	0.10

[a] Majority of the particles

[b] The largest particles

liquid-state ion exchange, the highest by solid-state ion exchange. The large amount of Ga in Ga^s/H-ZSM5 is consistent with the presence of Ga_2O_3, as identified by XRD. The content of Ga did not change significantly upon impregnation with Pt (entries 6–9, Table 1) or after sample regeneration (entry 10, Table 1). The Si/Al ratio remained more or less the same after impregnation with Pt (Si/Al = 24) or with Ga (Si/Al = 25). The content of Pt was between 1.8 and 2.6 wt% for all samples. The Pt content did not change upon reaction (entries 8 and 10, Table 1), indicating that leaching did not occur.

The BET surface area of the parent H-ZSM5 (entry 1, Table 1) was 400 m^2/g and decreased slightly upon modification with Pt (entry 2, Table 1) or Ga (entries 3 and 4, Table 1). After introduction of Ga by solid-state ion exchange (entry 3, Table 1) or liquid-state ion exchange (entry 4, Table 1), the microporous volume also decreased. Upon impregnation with Pt (entries 6–9, Table 1), the sorption properties of the samples did not change significantly. After regeneration (Pt/H-Ga^fZSM5r, entry 10), the BET surface area and the microporous volume of Pt/H-Ga^fZSM5 (entry 8) decreased slightly.

Figure 1 shows the TEM images of Pt/H-ZSM5 (a), Ga^i/H-ZSM5 (b), Ga^s/H-ZSM5 (c), Pt_b/H-Ga^fZSM5 (g), and Pt/H-Ga^fZSM5r (h) and STEM images of Pt/H-Ga^fZSM5 (d), PtGa^s/H-ZSM5 (e), and PtGa^i/H-ZSM5 (f). The TEM images of Pt/H-ZSM5 and Ga^i/H-ZSM5 reveal zeolite crystals and small dark spots, corresponding to the metal particles. The Pt particles (Fig. 1a) were ~1.6 nm and

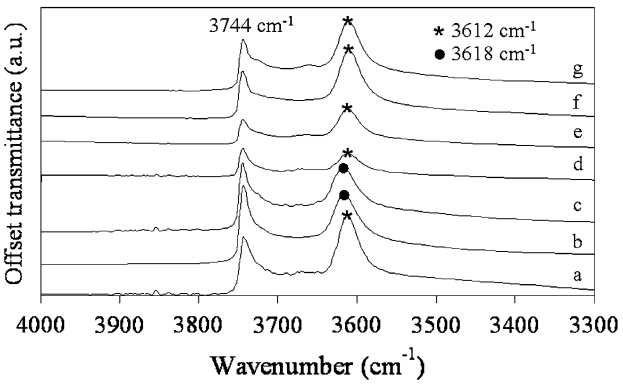

Fig. 2 FTIR spectra of H-ZSM5 (*a*), H-Ga^fZSM5 (*b*), Pt/H-Ga^fZSM5 (*c*), Ga^s/H-ZSM5 (*d*), PtGa^s/H-ZSM5 (*e*), Ga^i/H-ZSM5 (*f*), and PtGa^i/H-ZSM5 (*g*)

well-distributed. Ga is lighter than Pt, and, therefore, it was more difficult to detect the Ga particles (Fig. 1b). The average size of the Ga particles was 3.8 nm. Although a very large amount of Ga was present in the solid-state ion-exchanged sample, no Ga particles were observed in the TEM images (Fig. 1c). This indicates that Ga was present as large Ga_2O_3 particles, which we could not distinguish from the zeolite crystals on this scale and which were not found in the TEM images. The Pt particles, which were visible in STEM images, were 0.7 nm for Pt/H-Ga^fZSM5 (Fig. 1d) and about 1.0 nm for PtGa^s/H-ZSM5 (Fig. 1e) and PtGa^i/H-ZSM5 (Fig. 1f). Although the majority of the particles were smaller than 1 nm in all samples, some as large as

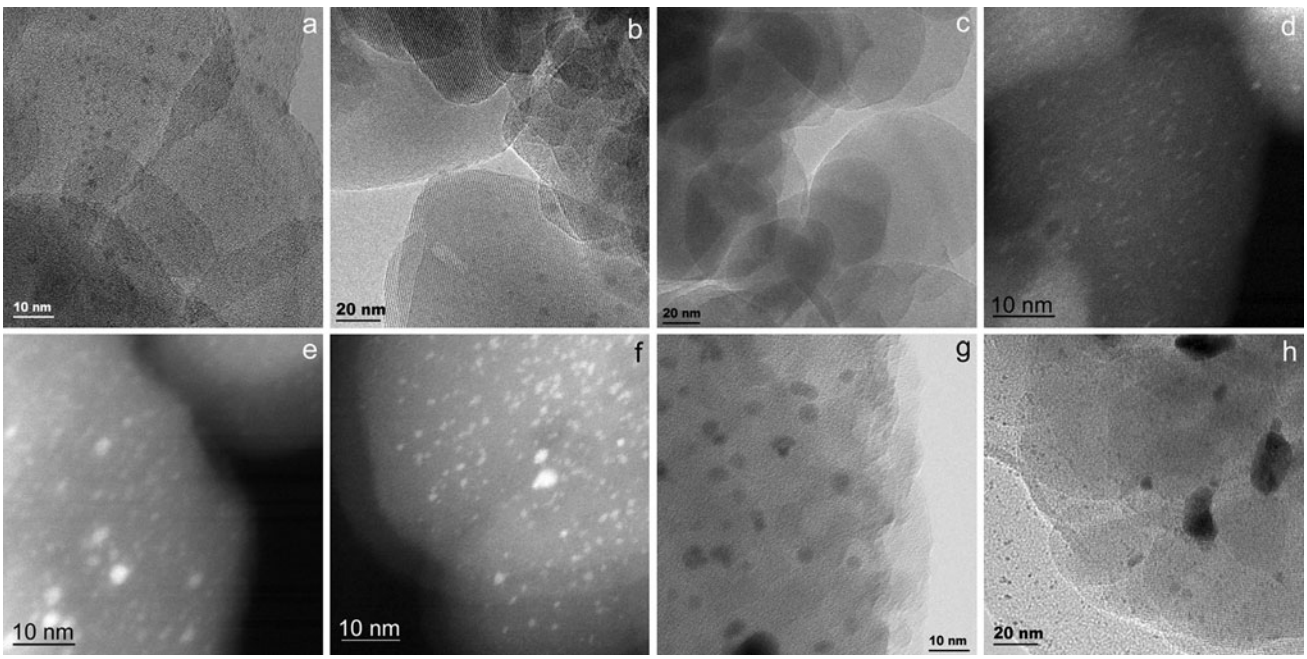

Fig. 1 TEM of Pt/H-ZSM5 (**a**), Ga^i/H-ZSM5 (**b**), Ga^s/H-ZSM5 (**c**), Pt_b/H-Ga^fZSM5 (**g**), and Pt/H-Ga^fZSM5r (**h**) and STEM of Pt/H-Ga^fZSM5 (**d**), PtGa^s/H-ZSM5 (**e**), and PtGa^i/H-ZSM5 (**f**)

Table 2 Results of alkylation over Ga- and PtGa-modified catalysts and Ga_2O_3

Entry	Sample	X^H (%)[a]	X (%)[b]	Selectivity (mol%)					Missing C (mol%)
				1PH[c]	2PH[d]	3PH[e]	bPH[f]	Cracking	
1	H-ZSM5	20	15	13	22	0	0	65	15
2	Pt/H-ZSM5	26	15	16	53	0	4	27	26
3	Ga^i/H-ZSM5	18	6	0	11	0	0	89	18
4	Ga^s/H-ZSM5	19	4	7	67	4	0	22	19
5	H-Ga^fZSM5	16	8	0	14	0	0	86	14
6	PtGa^i/H-ZSM5	24	9	16	39	0	10	35	24
7	PtGa^s/H-ZSM5	21	12	9	55	0	1	34	23
8	Pt/H-Ga^fZSM5	25	18	3	89	0	1	6	22
9	Pt_b/H-Ga^fZSM5	26	7	5	52	0	0	42	25
10	Pt/H-Ga^fZSM5r	12	10	2	77	4	3	15	26
11	Ga_2O_3	25	3	0	0	0	0	100	17

[a] Conversion of *n*-hexane

[b] Conversion of all hexane isomers

[c] 1-Phenylhexane

[d] 2-Phenylhexane

[e] 3-Phenylhexane

[f] Branched phenylhexanes

3–4 nm were present in PtGa^s/H-ZSM5 and PtGa^i/H-ZSM5, whereas the Pt particles over Pt/H-Ga^fZSM5 were all very small and well-distributed. The average Pt particle size of Pt_b/H-Ga^fZSM5 was 8.7 nm (Fig. 1g). After one reaction run and subsequent regeneration of the catalyst (Pt/H-Ga^fZSM5r, entry 10, Table 1), the Pt particle size increased from 0.7 over the fresh sample (Pt/H-Ga^fZSM5, entry 8, Table 1) to 1.0 nm (Fig. 1h). A few particles of 28 nm were detected in Pt/H-Ga^fZSM5r. The smallest particles remained well-distributed.

Figure S2 (supporting information) shows the ^{71}Ga MAS NMR spectra of H-Ga^fZSM5 and Ga^s/H-ZSM5. In the spectrum of H-Ga^fZSM5, there is one resonance at 159 ppm, indicating that most of the Ga was in the framework [20, 21]. A broad resonance between 50 and −100 ppm was also observed for H-Ga^fZSM5, indicating the presence of a small amount of extraframework Ga. Ga^s/H-ZSM5 showed no resonance at 159 ppm, whereas there was a broad peak at around 0 ppm, which is typical of extraframework Ga and which also appears in the spectrum of Ga_2O_3 [22]. This corresponded to the results obtained by XRD. Probably because of its low concentration, there was no clear signal of Ga for Ga^i/H-ZSM5, even after 48 h of measurement.

Figure 2 shows the OH stretching region of FTIR spectra of H-ZSM5, H-Ga^fZSM5, Pt/H-Ga^fZSM5, Ga^s/H-ZSM5, PtGa^s/H-ZSM5, Ga^i/H-ZSM5, and PtGa^i/H-ZSM5. There was one common intense band at 3744 cm^{-1}, corresponding to external silanol [23]. The band at around 3612 cm^{-1} in the spectra of H-ZSM5, Ga^s/H-ZSM5, PtGa^s/H-ZSM5, Ga^i/H-ZSM5, and PtGa^i/H-ZSM5 is typical of Brønsted acid sites (BAS), Si–(OH)–Al [23]. H-Ga^fZSM5 and Pt/H-Ga^fZSM5, containing framework Ga, showed a band at 3618 cm^{-1}, which corresponds to the stretching vibration of a hydroxyl bridging tetrahedrally coordinated framework Ga and Si, Ga–(OH)–Si [23, 27]. The normalized intensity of the band corresponding to the Brønsted acid sites decreased in the order H-ZSM5 > Ga^i/H-ZSM5 > PtGa^i/H-ZSM5 > H-Ga^fZSM5 > Pt/H-Ga^fZSM5 > PtGa^s/H-ZSM5 > Ga^s/H-ZSM5. Thus, ion-exchanged samples showed the lowest amount of Si–(OH)–Al, indicating that Ga ions exchanged the protons of the hydroxyl bridging groups. PtGa^i/H-ZSM5 and Pt/H-Ga^fZSM5 showed a similar intensity of the BAS-associated bands compared to Ga^i/H-ZSM5 and H-Ga^fZSM5.

3.2 Catalytic Experiments

Table 2 gives the results of alkylation of benzene with *n*-hexane over unmodified and Pt- and Ga-containing ZSM-5. Considerable conversion of *n*-hexane and benzene was reached over all catalysts. Alkylation, isomerization, and cracking products were detected. No olefins were observed. The isomerization products were 2- and 3-methylpentane. The alkylation fraction contained 1-, 2-, 3-, and branched phenylhexane. The conversion of benzene (not shown here) was similar to that of *n*-hexane, indicating that phenylalkanes resulted from both molecules [17]. The formation of the terminal product and a mechanistic study of the alkylation of benzene with *n*-hexane are described elsewhere [17]. Some cyclohexylbenzene, which was a product of two benzene molecules [17, 24–26], was detected in the

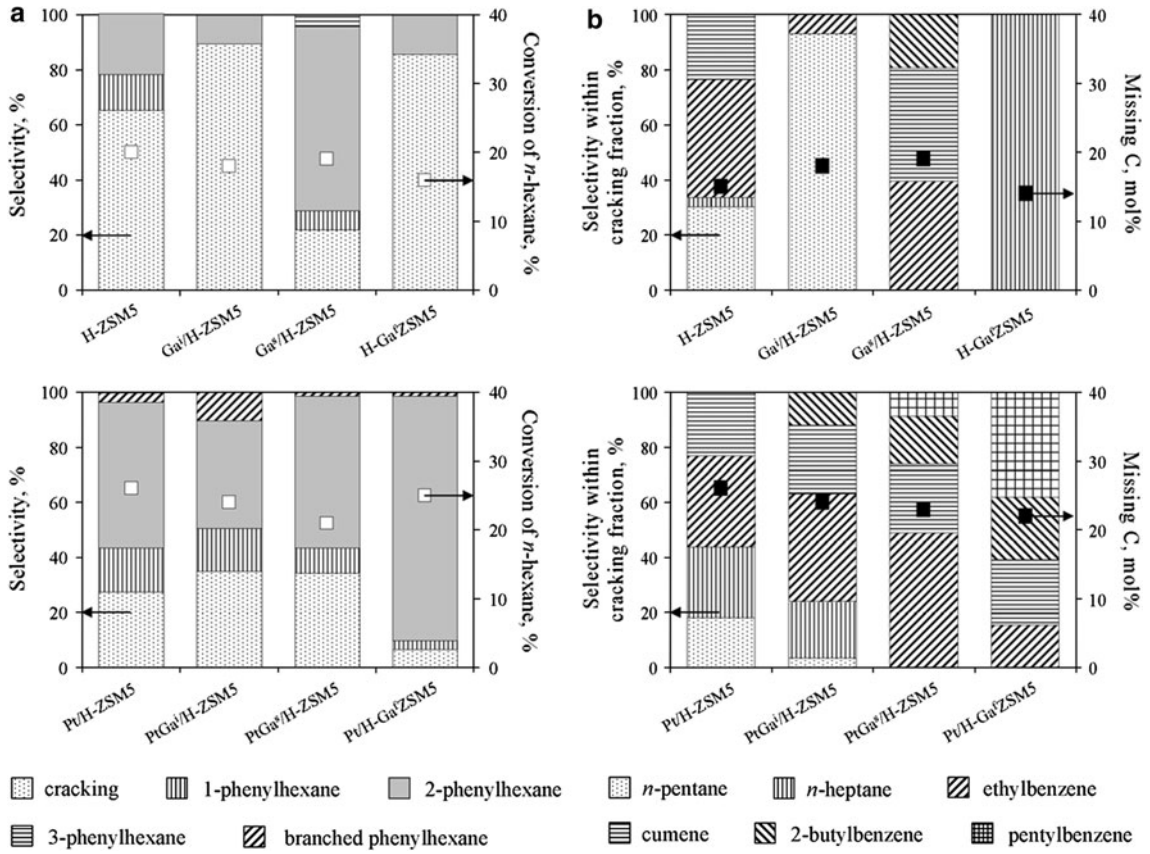

Fig. 3 **a** Product distribution (*bars*) and conversion levels (*open squares*) and **b** composition of the cracking fraction (*bars*) and missing carbon fraction (*filled squares*) in alkylation of benzene with *n*-hexane

product mixture. As cracking products we assigned *n*-pentane and *n*-heptane, which are the likely products of classical dimerization and cracking over the acid sites of the zeolite; ethylbenzene, cumene, butylbenzene, and pentylbenzene are the cracking products of phenylhexane. Cracking occurred over all catalysts. We analyzed the composition of the gas phase for several reactions. Hydrogen, methane, ethane, ethylene, propane, propylene, butane, and isopentane were detected. These light products were included to the fraction of "missing C", which varied between 15 and 26 mol% for different catalysts.

Over H-ZSM5 (entry 1, Table 2), the conversion of *n*-hexane was 20%. The liquid product phase contained 13% 1-phenylhexane, 22% 2-phenylhexane, and 65% cracked products. Impregnation with Pt (entry 2, Table 2) led to an increase in conversion to 26%, higher selectivity to alkylation, and suppressed cracking. The selectivity to 2-phenylhexane increased by about a factor of two, whereas the formation of 1-phenylhexane did not change. 4% branched phenylhexane formed.

Ga-modified samples showed similar activity; 16–19% *n*-hexane and 4–8% hexane isomers were converted. Over Ga^i/H-ZSM5 (entry 3, Table 2) with only 0.3 wt% of extra-framework Ga, only 11% 2-phenylhexane formed, the rest were cracking products. Over Ga^s/H-ZSM5 (entry 4, Table 2), containing 9.6 wt% extraframework Ga, 78% were alkylated products, 67% of which was 2-phenylhexane. Over H-Ga^fZSM5 (entry 5, Table 2) with Ga in the framework, 14% 2-phenylhexane and 86% cracking products formed.

The presence of Pt nanoparticles (entries 6–8, Table 2) led to an increase in conversion of *n*-hexane and its isomers. The conversion of hexane isomers was the highest (18%) over Pt/H-Ga^fZSM5 (entry 8, Table 2). Over PtGa^i/H-ZSM5 (entry 6, Table 2), conversion increased from 18 to 24%; and selectivity to 1- and 2-phenylhexane from 11 to 55%. Significant selectivity to branched phenylhexane (10%) was observed. Over PtGa^s/H-ZSM5 (entry 7, Table 2), the selectivity towards 2-phenylhexane decreased, whereas the selectivity to cracking increased from 22 to 34%. For Pt/H-Ga^fZSM5 (entry 8, Table 2), the selectivity to phenylhexanes increased from 14 to 93%, of which 89% was 2-phenylhexane. Compared to monometallic Pt- and Ga-containing samples, bimetallic PtGa-modified catalysts showed, in general, higher selectivity to alkylation products and isomerization and suppressed cracking. Ga_2O_3 (entry 9, Table 2) showed no selectivity to alkylation; isomerization and cracking products only were observed.

Figure 3b shows the composition of the cracking fraction of Pt- and Ga-modified samples and H-ZSM5. Note that only the products detected in the liquid-phase were quantified; light products and coke are represented by the "missing C". Over H-ZSM5, 30% *n*-pentane, 4% *n*-heptane, 43% ethylbenzene, and 24% cumene were formed. After the liquid-state ion exchange with Ga, 93% *n*-pentane and 7% ethylbenzene were found among the cracking products. Over Ga^s/H-ZSM5, ethylbenzene, cumene, and 2-butylbenzene formed. Only *n*-heptane was detected over H-Ga^fZSM5. After modification with Pt nanoparticles, the amount of *n*-pentane and *n*-heptane decreased, whereas more 2-butylbenzene and pentylbenzene were observed.

Figure 4 shows the time-evolution of the alkylation of benzene with *n*-hexane over Pt/H-Ga^fZSM5. At the beginning of the reaction, at conversions of *n*-hexane below 3%, only isomerization products of *n*-hexane and *n*-pentane and *n*-heptane were detected, which can all originate from the classical oligomerization, isomerization, and cracking. After 60 min, cumene started forming, followed by 2-phenylhexane at 150 min of reaction. The yield of methylpentanes, 2-phenylhexane, ethylbenzene, and cumene increased with time.

Over H-Ga^fZSM5-supported smaller Pt particles (0.7 nm, entry 8, Table 2), the conversion of hexane isomers was higher than over H-Ga^fZSM5-supported large particles (8.7 nm, entry 10, Table 2) of Pt. The selectivity in alkylation was 93% over Pt/H-Ga^fZSM5 and 57% over Pt_b/H-Ga^fZSM5. The sample with the smaller Pt particles showed higher selectivity to alkylaromatic products than the catalyst with larger particles. Only 6% cracking products were observed over Pt/H-Ga^fZSM5, whereas the selectivity to cracking over Pt_b/H-Ga^fZSM5 was 42%.

The catalytic stability of the sample was evaluated by comparing the catalytic activity and the product distribution over fresh Pt/H-Ga^fZSM5 (entry 8, Table 2) and recycled Pt/H-Ga^fZSM5r (entry 11, Table 2). The conversion over Pt/H-Ga^fZSM5r decreased to 12% compared to 25% over the fresh sample. Over Pt/H-Ga^fZSM5r, 12% less 2-phenylhexane and the double amount of cracking products formed.

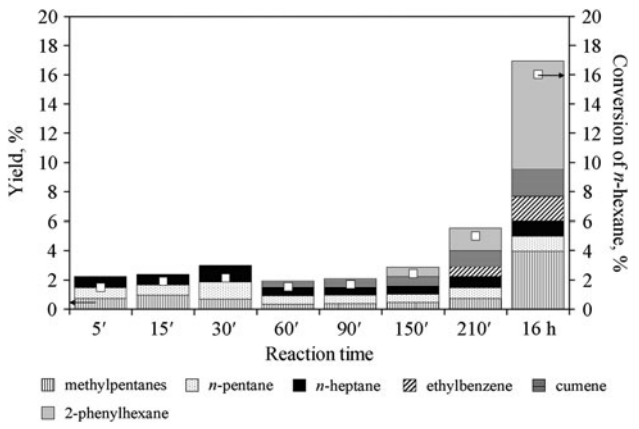

Fig. 4 Time-resolved study of the alkylation of benzene with *n*-hexane over Pt/H-Ga^fZSM5

4 Discussion

Benzene was alkylated with *n*-hexane, and up to 26% conversion of the alkane was reached at 205 °C under autogenous pressure and a benzene-to-*n*-hexane (B/H) ratio of one. We observed the formation of 1-, 2-, 3-, and branched phenylhexane as alkylation products. The maximum selectivity to alkylated products was 93%, 95% of which was 2-phenylhexane. Although alkylation already occurred over the parent H-ZSM5, its modification with Pt and Ga improved the selectivity to alkylation products. Similar effects were reported for alkylation of benzene with ethane [15, 16, 18, 19] and propane [8, 10, 11]. We assigned this increase in selectivity to phenylhexanes to the suppression of cracking and improved dehydrogenation of *n*-hexane over the metal. Considerable selectivity to alkylation products over the metal-free H-ZSM5 and its increase due to the introduction of the metal function suggest that 2- and 3-phenylhexanes were probably formed by two different mechanisms: the classical concerted mechanism and via the acid-catalyzed activation of benzene. These routes and the formation of the terminal product were discussed elsewhere [17].

Monometallic Ga-containing samples, obtained by solid-state and liquid-state ion exchange and containing Ga in extraframework positions, showed different catalytic performance, which can be explained by the very different Ga content. H-Ga^fZSM5, which contained Ga in the framework, showed low selectivity to alkylation products. This suggests that the Ga–(OH)–Si acid sites are catalytically inactive in alkylation. This is consistent with the conclusions reported in the literature [27]. However, we conclude that Ga_2O_3, too, is inactive in Ga^i/H-ZSM5 and Ga^s/H-ZSM5, because no alkylation was observed over the pure gallium oxide. The presence of acid sites and extraframework Ga is required for the formation of phenylhexanes, probably by the classical bifunctional mechanism.

It is interesting that, over H-Ga^fZSM5, modified with Pt nanoparticles, selectivity to phenylhexanes was very high, around 93%. 89% were 2-phenylhexane, the most desirable isomer. As mentioned before, the 2-isomer is the most biodegradable among all the phenylalkanes [1]. In the industrial Pacol and Detal processes, the selectivity to the 2-isomer reaches only 25% but at full conversion [1]. Modification of H-Ga^fZSM5 with Pt led to suppression of classical cracking reactions. The fact that the formation of *n*-heptane over H-Ga^fZSM5 was completely replaced by

the formation of ethylbenzene, cumene, butylbenzene, and pentylbenzene after introduction of Pt, points to the shift in the reaction pathway. Instead of oligomerization and cracking of dodecene, alkylation to phenylhexanes and their subsequent cracking is taking place. This effect was not observed to the same extent with the other Ga-containing samples, although the impregnation with Pt led to enhanced selectivity in alkylation. We suggest that the close proximity of very small Pt nanoparticles to framework Ga–(OH)–Si acid sites (in the micropores of ZSM-5) is the reason for this very high selectivity to 2-phenylhexane over Pt/H-Ga^{f}ZSM5.

Similar synergetic effects of Pt and Ga were suggested to be responsible for the enhanced selectivity in alkane aromatization [28, 29], steam reforming and dehydrogenation of methanol [30], dehydroizomerization of *n*-butane [31], hydrodechlorination of CCl_4 [32], and alkylation of benzene with propane [33]. Pt maintains a very low olefin concentration, suppressing cracking, while the close proximity of Pt to Ga–(OH)–Si is essential for the alkylation of benzene with the olefin intermediate. The limited pore size of ZSM-5 may be responsible for the preferential formation of 2-phenylhexane. Based on the very high selectivity to 2-phenylhexane, we speculate that there are almost no acid sites on the external surface.

Not only is the presence of the metal important for selective production of phenylhexanes, but also the size and distribution of the metal particles within the zeolite crystals. Over smaller Pt particles supported on H-Ga^{f}ZSM5, higher selectivity in alkylation and lower selectivity to cracked products were observed. Close proximity of metal and acid sites of the zeolite may explain the better selectivity over the small Pt particles. It may also explain the lower selectivity to phenylhexanes over the recycled Pt/H-Ga^{f}ZSM5r. The small Pt particles sintered during the reaction and did not redisperse with subsequent reduction of the catalyst, which led to the poorer catalytic performance compared to the fresh catalyst. Other studies mention aromatic alkylation with alkanes over bifunctional catalysts, but do not always give the size and dispersion of the metal particles, even they have a strong effect on the performance of the catalyst. The function of the acid and the metal must be balanced.

5 Conclusion

Alkylation of benzene with *n*-hexane over MFI zeolites was performed at moderate temperature (205 °C). Considerable conversion and high selectivity to phenylhexanes were reached after modifying ZSM-5 with Ga and Pt. The presence of these metals suppressed cracking. The coexistence of Ga and acid sites of the zeolite resulted in enhanced isomerization of *n*-hexane to methylpentanes. The nature of the Ga species (framework and extraframework) played an important role in the catalytic performance. Low activity and selectivity was observed for the monometallic sample containing only framework Ga. After modification with very small Pt nanoparticles, selectivity to 2-phenylhexane was high (89%), and considerable conversion of *n*-hexane ($\sim$25%) was observed. We found that catalytic performance depends on the Pt particle size. Reaction over smaller Pt particles led to higher selectivity in alkylation and suppressed cracking and multialkylation. We suggest that the close proximity of Ga–(OH)–Si acid sites in the micropores of H-Ga^{f}ZSM5 and small particles of Pt lead to very high selectivity of Pt/H-Ga^{f}ZSM5 to 2-phenylhexane.

Acknowledgments The work was supported by the Swiss National Science Foundation. The authors thank Dr. Frank Krumeich and the Electron Microscopy Centre of the ETH Zurich (EMEZ).

References

1. Kocal JA, Vora BV, Imai T (2001) Appl Catal A 221:295
2. Borutskii PN, Kozlova EG, Podkletnova NM, Gil'chenok ND, Sokolov BG, Zuev VA, Shatovkin AA (2007) Petrol Chem 47:250
3. Pujado PR (1996) In: Meyers RA (ed) Linear alkylbenzene manufacturer: handbook of petroleum refining processes. McGraw-Hill, New York, p 1.53
4. Kocal JA (1993) US Patent 5,196,574 to UOP
5. Olah GA, Schilling P, Staral JS, Halpern Y, Olah JA (1975) J Am Chem Soc 97:6807
6. Smirniotis PG, Ruckenstein E (1995) Ind Eng Chem Res 34:1517
7. Ivanova I, Blom N, Derouane EG (1996) J Mol Catal A 109:157
8. Smirnov A, Mazin E, Yuschenko V, Knyazeva E, Nesterenko S, Ivanova I, Galperin L, Jensen R, Bradley S (2000) J Catal 194:194
9. Abasov SI, Babayeva FA, Zarbaliyev RR, Abbasova GG, Tagiyev DB, Rustamov MI (2003) Appl Catal A 251:267
10. Todorova S, Su B (2004) Catal Today 93–95:417
11. Bigey C, Su B (2004) J Mol Catal A 209:179
12. Sealy S, Traa Y (2005) Appl Catal A 294:273
13. Huang X, Sun X, Zhu S, Liu Z (2007) Catal Lett 119:332
14. Bressel A, Donauer T, Sealy S, Traa Y (2008) Microporous Mesoporous Mater 109:278
15. Lukyanov DB, Vazhnova T (2008) J Catal 257:382
16. Lukyanov DB, Vazhnova T (2008) J Mol Catal A 279:128
17. Danilina N, Payrer EL, van Bokhoven JA (2010) Chem Commun 46:1509
18. Kato S, Nakagawa K, Ikenaga N, Suzuki T (1999) Chem Lett 207
19. Alireza S, Rezai S, Traa Y (2008) Catal Lett 122:91
20. Bayence CR, van Hooff JHC, Kentgens APM, de Haan JE, van de Ven LJM (1989) Chem Commun 1292
21. Timken HKC, Oldfield E (1987) J Am Chem Soc 109:7669
22. O'Dell LA, Savin SLP, Chadwick AV, Smith ME (2007) Appl Magn Reson 32:527
23. Post MFM, Huizinga T, Emeis CA (1989) In: Karge HG, Weitkamp J (eds) Zeolites as catalysts, sorbents and detergent builders. Elsevier, Amsterdam
24. Slaugh LH (1968) Tetrahedron 24:4523

25. Borodina IB, Ponomareva OA, Fajula F, Bousquet J, Ivanova II (2007) Microporous Mesoporous Mater 105:181
26. Jun Q, Komura K, Kubota Y, Sugi Y (2007) Chin J Catal 28:246
27. Fricke R, Kosslick H, Lischke G, Richter M (2000) Chem Rev 100:2303
28. Shpiro ES, Shecchenko DP, Tkachenko OP, Dmitriev RV (1994) Appl Catal A 107:147
29. Shpiro ES, Shecchenko DP, Dmitriev RV, Tkachenko OP, Minachev KM (1994) Appl Catal A 107:165
30. Iwasa N, Takezawa N (2003) Top Catal 22:215
31. Vieira A, Tovar MA, Pfaff C, Betancourt P, Mendez B, Lopez CM, Machado FJ, Goldwasser J, Ramirez de Agudelo MM (2000) Stud Surf Sci Catal 130:269
32. Cao YC, Jiang XZ (2005) J Mol Catal A 242:119
33. Todorova S, Su B (2003) J Mol Catal A 201:223